Journal of Biomedical Optics

BiomedicalOptics.SPIEDigitalLibrary.org

In vivo measurement of tissue oxygenation by time-resolved luminescence spectroscopy: advantageous properties of dichlorotris(1, 10-phenanthroline)-ruthenium(II) hydrate

Veronika Huntosova
Sandrine Gay
Patrycja Nowak-Sliwinska
Senthil Kumar Rajendran
Matthieu Zellweger
Hubert van den Bergh
Georges Wagnières

SPIE.

In vivo measurement of tissue oxygenation by time-resolved luminescence spectroscopy: advantageous properties of dichlorotris(1, 10-phenanthroline)-ruthenium(II) hydrate

Veronika Huntosova,[a,†] Sandrine Gay,[a] Patrycja Nowak-Sliwinska,[a,b] Senthil Kumar Rajendran,[a] Matthieu Zellweger,[a] Hubert van den Bergh,[a] and Georges Wagnières[a,*]
[a]Swiss Federal Institute of Technology (EPFL), Institute of Chemical Sciences and Engineering, Station 6, CH-1015 Lausanne, Switzerland
[b]University Hospital (CHUV), Department of Urology, BH-10, Rue du Bugnon 46, CH-1011 Lausanne, Switzerland

Abstract. Measuring tissue oxygenation *in vivo* is of interest in fundamental biological as well as medical applications. One minimally invasive approach to assess the oxygen partial pressure in tissue (pO_2) is to measure the oxygen-dependent luminescence lifetime of molecular probes. The relation between tissue pO_2 and the probes' luminescence lifetime is governed by the Stern-Volmer equation. Unfortunately, virtually all oxygen-sensitive probes based on this principle induce some degree of phototoxicity. For that reason, we studied the oxygen sensitivity and phototoxicity of dichlorotris(1, 10-phenanthroline)-ruthenium(II) hydrate [Ru(Phen)] using a dedicated optical fiber–based, time-resolved spectrometer in the chicken embryo chorioallantoic membrane. We demonstrated that, after intravenous injection, Ru(Phen)'s luminescence lifetime presents an easily detectable pO_2 dependence at a low drug dose (1 mg/kg) and low fluence (120 mJ/cm^2 at 470 nm). The phototoxic threshold was found to be at 10 J/cm^2 with the same wavelength and drug dose, i.e., about two orders of magnitude larger than the fluence necessary to perform a pO_2 measurement. Finally, an illustrative application of this pO_2 measurement approach in a hypoxic tumor environment is presented. [DOI: 10.1117/1.JBO.19.7.077004]

Keywords: biodistribution; *in vivo*; luminescence lifetime; oxygen partial pressure; phototoxicity; dichlorotris(1, 10-phenanthroline)-ruthenium(II) hydrate.

Paper 140196R received Mar. 25, 2014; revised manuscript received May 23, 2014; accepted for publication Jun. 5, 2014; published online Jul. 18, 2014.

1 Introduction

The noninvasive measurement of tissue oxygenation is challenging and has been addressed by numerous research groups for decades.[1,2] Tissue hypoxia can be caused by a number of factors, e.g., low oxygen partial pressure (pO_2) in arterial blood (due to pulmonary disease or high altitude), reduced ability of blood to carry oxygen (as a result of anemia, methemoglobin formation, carbon monoxide poisoning, reduced tissue perfusion), inability of cells to use oxygen because of intoxication, or other factors.[3] Tissue oxygenation is also relevant for some therapeutic approaches, such as radiotherapy, where microcirculation and adequate oxygen supply are major success factors:[4] it was reported that nearly triple radiation dose is needed to kill hypoxic cells as compared to normal aerobic cells.[5] Prognosis for survival and recurrence-free survival of patients with hypoxic tumors is significantly shorter[6] than for patients with nonhypoxic tumors. The measurement of tissue oxygenation is, therefore, of great clinical interest not only to measure tumor oxygenation, but also as a predictive assay for future treatment development and diagnostics (radiotherapy, chemotherapy, photodynamic therapy).[7,8] It should be noted that measuring pO_2 also provides valuable fundamental information regarding tissue respiration.[9]

During the last decades, two main methods have been used for pO_2 measurements in tissue: Eppendorf polarographic needle electrodes and optical fiber–based sensors.[10,11] Both methods are based on the use of needles or interstitial catheters with diameters on the order of several hundreds of microns. Consequently, *in vivo* measurements with these methods induce tissue damage or modification. Following the development of sensitive and noninvasive time-resolved optical spectroscopic techniques based on the oxygen-dependent luminescence quenching of molecular probes, a third method is now available, whereby the level of oxygenation can be measured quantitatively and minimally invasively at selected sites.[12–14] Time-resolved luminescence detection techniques to measure pO_2 are, in general, more reliable than luminescence intensity-based methods, because luminescence lifetime does not depend on the concentration of a probe.[15,16] Unfortunately, most of these luminescent oxygen probes are phototoxic, due to the production of singlet oxygen in the quenching process of their triplet state.[17] This phototoxicity leads to tissue damage, including vascular damage, during the pO_2 measurements.[12]

Luminescent complexes of transition metals, i.e., Ru(II), Os (II), Rh(III), Ir(III), and Pt(II), are very promising pO_2 sensors. They display useful properties, such as long luminescence

*Address all correspondence to: Georges Wagnières, E-mail: georges.wagnieres@epfl.ch

†Current affiliation: P.J. Safarik University, Centre for Interdisciplinary Biosciences, Faculty of Science, Jesenna 5, 041 54 Kosice, Slovakia

0091-3286/2014/$25.00

lifetimes, high luminescence quantum yields, high extinction coefficients in the visible range, and good chemical, thermal, and photochemical stabilities.[18,19] Following preliminary studies indicating that the ruthenium organometallic complex dichlorotris(1, 10-phenanthroline)-ruthenium(II) hydrate [Ru(Phen)] (see chemical structure in Fig. 1) presents both a limited phototoxicity and oxygen-dependent luminescence lifetimes, we decided to study it *in vivo* for pO_2 measurements, thus expanding on prior studies in liquids.[20–22] Ru(Phen) presents three main absorption bands, shown in Fig. 1. The first and most intense band (262 nm) is due to the 1,10-phenanthroline ligand $\pi - \pi*$ transition, the broad band located between 350 and 500 nm is due to the $d_\pi - \pi*$ metal-to-ligand charge transfer, and the smallest one at 684 nm corresponds to the metal *d-d* transition.[23,24] The broad emission of this complex at 600 nm (see Fig. 1) can be efficiently quenched by oxygen. It is assigned to a phosphorescence process resulting from a metal-to-ligand charge transfer.[24] This emission band is very bright and highly photostable.[25]

Ru(Phen) is a complex cation, which does not have specific active groups. Biological activity of such compounds is a function of the cation as a whole and not of the metallic atom.[26] Antitumoral and virostatic action of Ru-based polypyridyl complexes was observed both *in vivo* and *in vitro* 50 years ago.[27–30] Ru(Phen) is modestly cytotoxic ($IC_{50} \sim 90$ μmol/l) and possesses relatively high clearance rate *in vivo*.[31–33] In general, *in vivo* toxicity strongly depends on the way of Ru(Phen) administration. Minimum lethal doses of Ru(Phen) in mice are 6.6 mg/kg, when administered by intraperitoneal injection.[32] In another study, intravenous injection of Ru(Phen) between 4 and 16 mM/kg in rats frequently led to a drop in heart rate and respiratory arrest. A fast decrease of Ru(Phen) concentration in the bloodstream due to a high renal clearance rate was also observed.[33] Interestingly, there was neither any toxic effect observed after per os administration of ^{103}Ru(Phen) in digestion studies with sheep, nor any disruption of metabolic activity of the rumen microbiota.[34] Apart from a few references to a minimal phototoxicity of Ru(Phen) during the measurements, no *in vivo* or *in vitro* phototoxicity tests have been published to the best of our knowledge.[35,36]

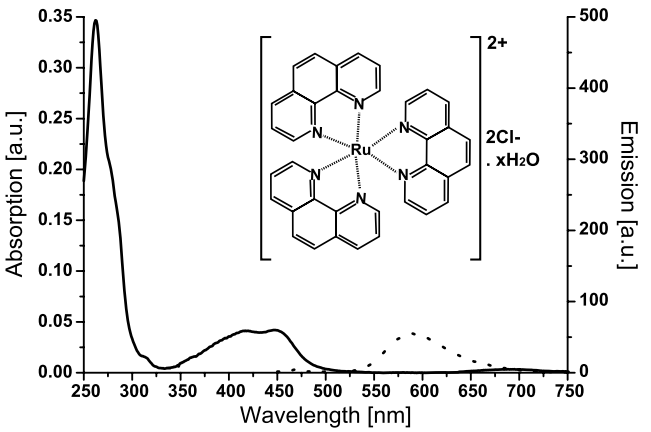

Fig. 1 Absorption (solid line) and emission spectrum (dotted line, excitation = 470 nm) of dichlorotris(1, 10-phenanthroline)-ruthenium (II) hydrate [Ru(Phen)] (1 and 0.01 mg/ml, respectively) in 0.9% NaCl isotonic solutions. Drawing of Ru(Phen)'s molecular structure is inserted.

In the present study, we have quantified the phototoxicity of Ru(Phen) *in vivo* after intravenous injection. The model we used for this purpose is the chicken chorioallantoic membrane (CAM), a model widely used in preclinical studies of the microvasculature.[37–39] In addition, we report the first *in vivo* measurement of tissue pO_2 based on the time-resolved detection of Ru (Phen) luminescence. These measurements have been performed using a unique optical fiber-based, time-resolved spectrometer developed in our laboratory.[40] Our study demonstrates that the fluence necessary to perform a tissue pO_2 measurement is lower than the phototoxic threshold by about two orders of magnitude. This avoids any possible photoinduced vascular effects. Finally, an illustrative application of this approach to measure intratumor oxygenation is presented in human tumors xenografted on CAM.

2 Materials and Methods

2.1 *Chemicals*

2.1.1 *Ru(Phen)*

Dichlorotris(1, 10-phenanthroline)-ruthenium(II) hydrate powder of 98% purity (Sigma-Aldrich, St. Louis, Missouri) was dissolved in a sterile solution (0.9% NaCl isotonic solution, Bichsel AG, Switzerland).

2.1.2 *Oxyphor R0*

Pd-meso-tetra(4-carboxyphenyl)porphyrin (PdTCPP) powder of 95% purity (Oxygen Enterprises Ltd., Philadelphia, Pennsylvania) was dissolved in 0.9% NaCl solution at pH 9.0, and the pH was adjusted to pH 7.4 with 0.1% HCl.

2.1.3 *Fluorescein isothiocyanate-dextran*

Fluorescein isothiocyanate-dextran (FITC-dextran; 20 kDa powder; Sigma-Aldrich) was dissolved in NaCl isotonic solutions to the final concentration of 25 mg/ml.

2.1.4 *Coumarin 102*

Laser dye powder coumarin 102 (Lambdachrome®, Acton, Massachusetts) was dissolved in 99.9% pure methanol at 1.44 g/l.

2.1.5 *Gas mixtures*

Pure nitrogen gas (Carbagas, Switzerland) was mixed in The BRICK—gas mixer (Life Imaging Services GmbH, Switzerland) with air to reach gas mixtures at nominal oxygen concentrations of 0, 5, 10, 15, and 21% M/M (corresponding pO_2: 0, 37, 74, 111, and 155.4 mm Hg).

2.2 *Chicken Embryo Chorioallantoic Membrane Preparation*

Fertilized chicken eggs (Animalco AG, Switzerland) were transferred into an automatic turn incubator (FIEM snc, Italy). Eggs were incubated blunt end up during 3 days at 37°C, at 65% of relative humidity and at atmospheric oxygen pressure (155.4 mm Hg). On the third embryo development day (EDD), a small part of the shell on the pointed end was removed creating a hole (~3 mm in diameter), which was then covered by tape (Scotch® Magic™, St. Paul, Minnesota). Eggs were

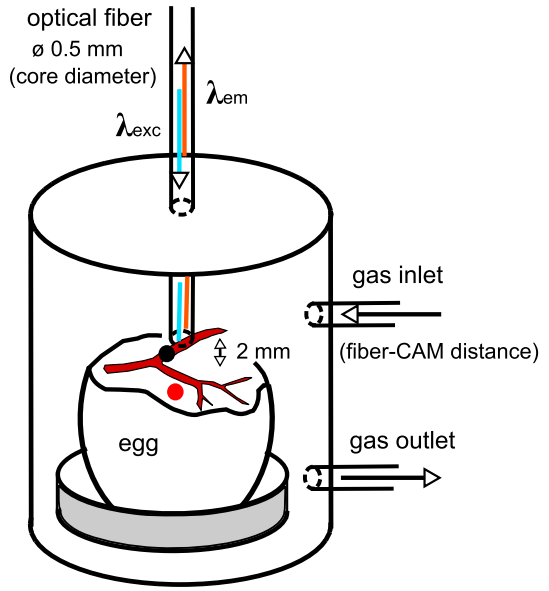

Fig. 2 Schematic representation of *in vivo* sample part of the time-resolved luminescence lifetime experimental setup for oxygen partial pressure (pO_2) measurement. Egg is inserted in the closed gas chamber with the optical fiber perpendicularly positioned 2 mm above chorioallantoic membrane (CAM). The gas exchange occurs through the inlet and the outlet of the gas. Irradiation (λ_{exc}) and detection (λ_{em}) is carried out with the same optical fiber from 1-mm^2 spot. Two main areas of interest are defined: (a) intravascular compartments (200 μm < vessels), indicated with black circle, and (b) extravascular compartments (vessels < 100 μm), indicated with red circle (red circle appears gray in BW figure).

then returned into the incubator blunt end down in a static position until used. At EDD 11, the hole in the shell was enlarged to ~2.5 cm in diameter, enabling easy CAM observation. Each treated CAM was placed either under an epifluorescence microscope Nikon eclipse E 600 FN (Nikon, Japan) or into the gas chamber (see Fig. 2) for further measurements and processing.

2.3 *CAM-Tumor Model Preparation*

Human A2780 ovarian carcinoma cells were used to establish tumor xenografts onto the CAM, as described in previous studies.[41] Briefly, tumor cells were suspended in an RPMI-1640 medium, GlutaMAX™ (Gibco, United Kingdom) supplemented with 10% fetal bovine serum, 1% penicillin/streptomycin, and containing 20% methocel (Sigma-Aldrich). Several 50-ml drops (1×10^6 cells/drop) were dispensed on the internal part of the lid of a Petri dish and were incubated in a humid atmosphere containing 5% CO_2 at 37°C in the dark. After 24 h, spheroids were harvested and placed on the CAM (EDD 7). CAM were prepared as described above until EDD 7; the hole in the shell was enlarged in order to provide better access for spheroids placement. CAM with spheroids was incubated at 37°C, 65% relative humidity, and atmospheric oxygen pressure (155.4 mm Hg) until used. The size of tumor xenografts was estimated and ~3 × 3 mm spheroids were used for further measurements (see Fig. 3).

2.4 *Absorption and Luminescence Spectroscopy of Ru(Phen)*

Absorption and fluorescence spectroscopy were used to determine the optimal conditions for Ru(Phen) *in vivo* observation.

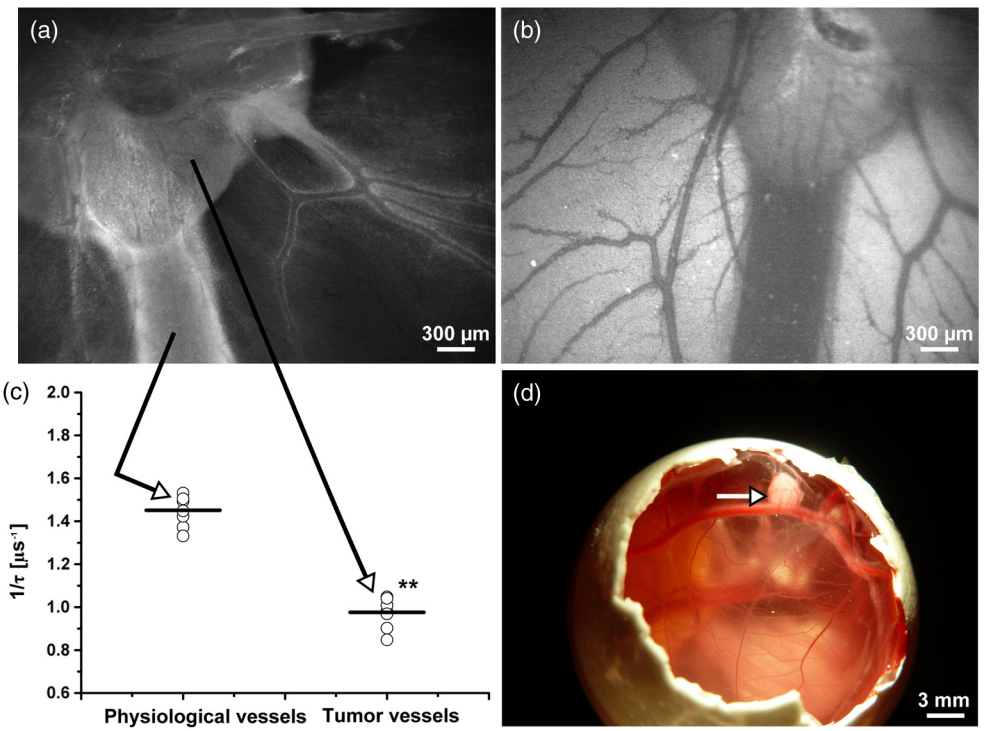

Fig. 3 (a) Representative luminescence angiography of CAM with the tumor 10 min after Ru(Phen) (10 mg/kg) intravenous injection and (b) before Ru(Phen) administration. (c) Ru(Phen) reciprocal lifetimes determined in the physiological and tumoral vessels. (**$p < 0.001$, seven eggs). Physiological and tumoral vessels are denoted with corresponding arrows. (d) Low-magnification (1.6×) white light image of the CAM presents a grafted tumor marked by the arrow.

All measurements were performed in 3-ml (1 cm of optical path length) quartz cuvettes (Hellma, Germany) at room temperature (25°C) and at atmospheric pO_2 (155 mm Hg). Absorption spectra of 1 mg/ml Ru(Phen) in 0.9% NaCl isotonic solution in the range of 250 to 750 nm (2-nm slits, 1-nm step) were collected with a CARY 500 Scan/UV-Vis-NIR spectrophotometer (VARIAN, Australia).

The luminescence spectrum of 0.01 mg/ml Ru(Phen) in NaCl isotonic solution was measured by a FluoroLog® spectrophotometer (Horiba Jobin Yvon, Germany) equipped with a xenon short-arc lamp to produce an excitation at 470 nm (3-nm slit). The Ru(Phen) emission was detected between 480 and 750 nm (3-nm slit, 1-nm step).

2.5 *Ru(Phen) Pharmacokinetics and Biodistribution in CAM*

Ru(Phen) pharmacokinetics measurements in CAM were performed as described in previous studies.[37] Briefly, 20 μl of solution containing 10 mg/kg of Ru(Phen) were injected under the microscope (within 5 s) into the main vein of CAM. Ru(Phen) excitation was performed by a Hg-arc lamp (HBO 103 W/2, Osram, Germany) filtered at 470 ± 20 nm. Excitation and Ru (Phen) emission were separated by a 505-nm dichromatic mirror, and a long-pass emission filter at 520 nm was used to reject all excitation light. Images showing the Ru(Phen) luminescence were recorded 10 min after intravenous injection at regular 1-min intervals. These images of the CAM surface were recorded with a digital scientific camera (PCO.1300, PCO Imaging, Germany) and a low-magnification objective (4X/0.13, Plan Fluor $\infty/-$, Nikon, Japan) as a function of time, with 100-ms exposure. Ru(Phen) luminescence radiance inside the blood vessels (I_{in}) with respect to the extravascular tissues (I_{out}) enables determination of the normalized photographic contrast C_{phot} according to Eq. (1):

$$C_{phot} = [I_{in} - I_{out}]/[(I_{in} + I_{out}) \times C_{phot,max}], \quad (1)$$

where $C_{phot,max}$ represents the highest photographic contrast. This photographic contrast was determined for areas corresponding to the center and the walls of the vessels (see Fig. 4). Ru(Phen) luminescence radiance measurements were performed by analyzing the signal recorded along a profile perpendicular to the vessel axis using the Image J software (National Institutes of Health, Bethesda, Maryland). These measurements have been performed for vessels (mainly veins) presenting five different diameters ranging between 50 and 500 μm. One point presented in the pharmacokinetics curve (see Fig. 4) corresponds to the average value of measurements performed with three different eggs.

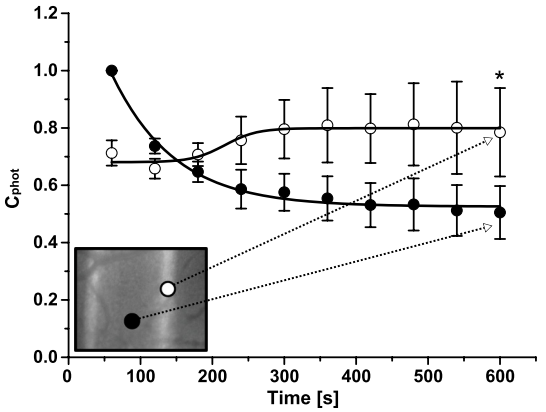

Fig. 4 Pharmacokinetics of Ru(Phen) during 10 min following intravenous injection defined by photographic contrast (C_{phot}) in Eq. (1). An insert figured biodistribution of Ru(Phen) 10 min after injection (see Fig. 7). White circles correspond to C_{phot} assessed in the wall of the blood vessels as displayed in the inserted picture. Black circles correspond to C_{phot} estimated in the intravascular space (see insert). (*$p = 0.0408$).

Vascular luminescence imaging and spectroscopy of photosensitive drugs is often strongly influenced by the hemoglobin contained in the bloodstream. This pigment strongly absorbs below 600 nm, with a maximum at 405 nm.[42] We minimized this hemoglobin absorption effect *in vivo* by using an excitation wavelength at 470 nm, which is a compromise between light transmission trough small vessels and Ru(Phen) excitation (Fig. 1).

2.6 *Acute Dark Toxicity of Ru(Phen)*

Twenty-microliter solutions containing different amounts of Ru (Phen) corresponding to doses of 1, 5, 10, 50, 100, and 200 mg/kg were injected intravenously to the CAM in the dark. At least six eggs were injected for each Ru(Phen) dose applied. Eggs were returned to the incubator and maintained in the dark. Acute dark toxicity was evaluated 24, 48, and 72 h after injection as the number of eggs that did not survive.

2.7 *Ru(Phen) Phototoxicity Assessment*

On EDD 11, eggs were placed under the microscope and a treatment area was defined by placing a small plastic ring (8 mm in diameter; thickness: 1 mm) on the CAM membrane. The purpose of this plastic ring was to facilitate the identification of the illuminated spot 24 h after the treatment. Prior to injection of Ru (Phen), an autofluorescence image of the CAM surface was recorded. Subsequently, Ru(Phen) was injected *in situ* under the microscope at doses ranging between 1 and 20 mg/kg. Irradiation of the 2.2-mm^2 treated area was performed with the same microscope and filter set as described above in the biodistribution study, with an irradiance of 64 mW/cm^2. The fluence was 1, 2, and 10 J/cm^2 (corresponding to irradiation times of 16, 32, and 160 s), and the drug-light interval (DLI) was 1 or 10 min. Eggs were returned to the incubator and incubated in the dark until the following day.

The evaluation of Ru(Phen) phototoxicity was based on the vascular damages induced on the CAM membrane 24 h after irradiation. The status of the vessels was controlled by injecting 20 μl of FITC-dextran solution in the vein and performing a fluorescence angiography 1 min after the injection. The spectral design of the microscope was not changed for this angiography. One milliliter of black ink (Parker, France) was injected into the extra-embryonic cavity of CAM to screen the autofluorescence produced by deep-seated tissues. The diameter of the vessels was measured with the Image J software. This distance in pixels was recalculated and used as the scale displayed in Fig. 5. The diameter of the largest closed vessel was measured and used as an index of vascular damage range between 0 and 5, as described in detail in previous publications.[37,38] The minimal value "0" refers to no detectable photodamage to the vasculature. Closure of the smallest visible blood vessels (diameter 5 to 10 μm) was termed grade 1, closure of the vessels with a diameter ranging between 10 and 30 μm grade 2, closure of the vessels with a diameter ranging between 30 and 70 μm

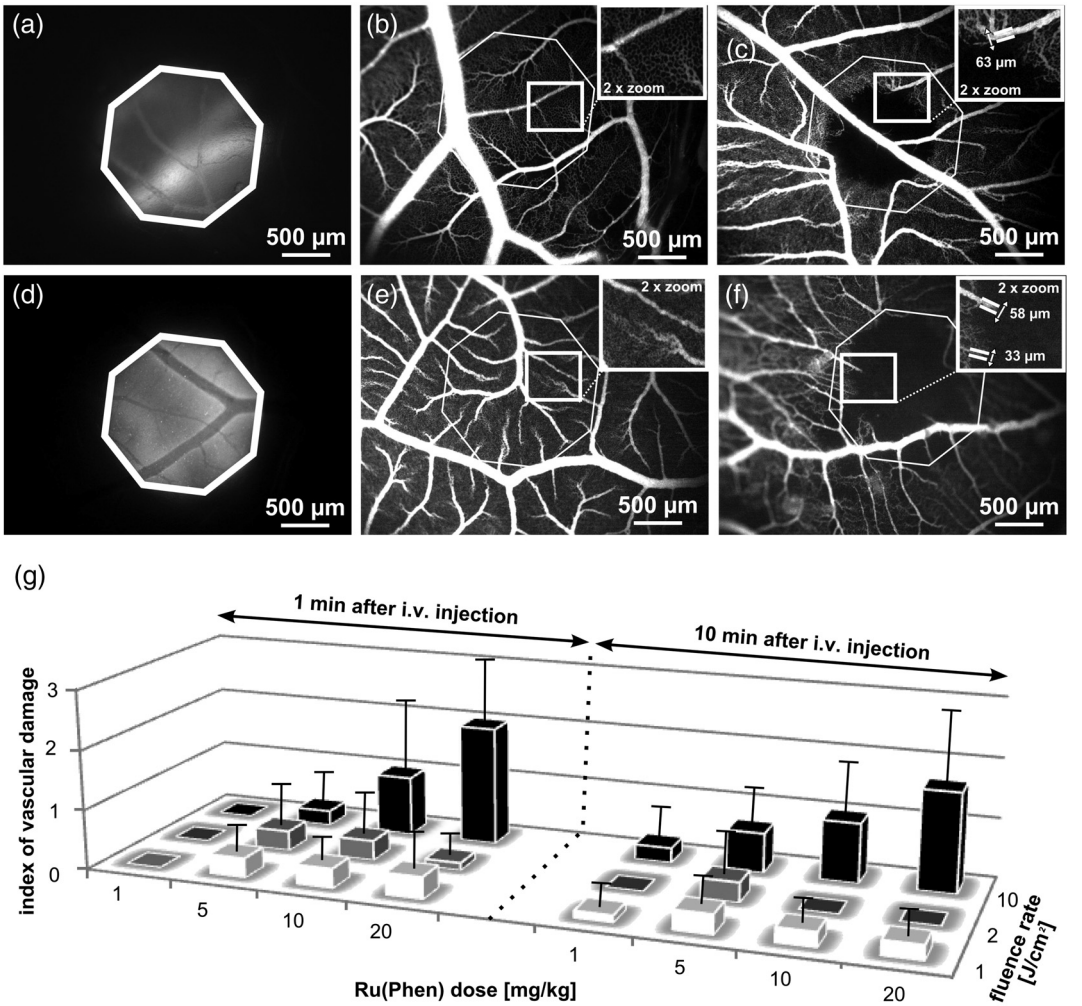

Fig. 5 Phototoxic effects induced by Ru(Phen) on the CAM blood vessels for drug-light intervals (DLIs) of 1 and 10 min. Typical luminescence angiography of 20 mg/kg Ru(Phen) performed (a) 1 min and (d) 10 min after injection before irradiation. The diameter of the illuminated area is 2 mm. Fluorescence angiography of fluorescein isothiocyanate-dextran performed 24 h after illumination with (b) 1 J/cm^2, DLI 1 min, index of vascular damage "0," (c) 10 J/cm^2, DLI 1 min, index of vascular damage "3," (e) 1 J/cm^2, DLI 10 min, index of vascular damage "0," (f) 10 J/cm^2, DLI 10 min, index of vascular damage "3," (excitation at 470 ± 20 nm). (g) Three-dimensional graphs reporting the index of vascular damage induced by different light and Ru(Phen) doses ranging between 1 to 10 J/cm^2 and 1 to 20 mg/kg, respectively. Four eggs were treated per condition. Error bars represent the standard deviations of a confidence interval 68%. See also Sec. 2 for more details.

grade 3, and closure of the vessels with diameter 70 μm and partial closure of larger vessels grade 4. A total occlusion of the irradiated area was assigned grade 5. These data were plotted in three-dimensional graphs (vascular damages × fluence × drug dose). The average values and standard deviations obtained with four eggs are presented in such graphs (see Fig. 5).

2.8 *Luminescence Lifetime Spectrometer and Signal Processing*

Luminescence lifetime of Ru(Phen) was measured with a dedicated optical fiber-based, time-resolved spectrometer developed in our laboratory and described in detail in previous publications.[40] Briefly, this compact setup consists of a nitrogen laser-pump and tunable dye (coumarin 102) laser emitting at 470 nm (pulse duration: <10 ns; repetition range: 10 Hz). The laser light is coupled into a single optical fiber (500 μm core diameter) that probes the sample. The same fiber was used to collect the sample luminescence. This luminescence was filtered by an emission filter [660 to 735 nm (HQ 700/75 M] and detected by a gateable photomultiplier. This spectral design was defined so that most of the tissue autofluorescence (observable with this CAM model in the range of 600 to 650 nm) was rejected, while an important proportion of Ru (Phen) luminescence was detected. In addition, the photomultiplier was maintained in the "off" mode during the first 2 μs after the laser pulse to prevent its saturation and loss of dynamic range due to the tissue autofluorescence. Detected light was transformed by the photomultiplier into an analog electrical signal, which was supplied to a digital storage oscilloscope for acquisition and processing. Fifty sweeps were measured over

the whole range, with equal intervals, digitized in 24-bit floating point values and transferred to a personal computer for further analysis. The resulting decay time reported in our paper corresponds to an average of these 50 sweeps. Ru(Phen) luminescence lifetimes were obtained by fitting the time-dependent digitized signal with a mono-exponential function.

$$f(t) = A.e^{t/\tau}, \tag{2}$$

where $f(t)$ is the time-dependent digitized signal, A is the pre-exponential factor that is proportional to Ru(Phen) luminescence intensity, t is the time after the laser pulse, and τ is the luminescence lifetime of Ru(Phen).

The Levenberg-Marquardt method has been used for nonlinear least-squares fit of the measured signal. The quality of the fits was graphically checked by plotting the residuals as well as their autocorrelation.

2.9 pO_2 Measurements Based on Ru(Phen) Luminescence Lifetime

2.9.1 Measurements in solution

On EDD 11, 300 μl of blood were carefully drawn from the vein of CAM and placed in a conical microcentrifuge tube with anticoagulant (ethylenediaminetetraacetic acid, Eppendorf®, Hauppauge, New York). A fraction of CAM blood (150 μl) was separated by centrifugation (1 min, 1200 rpm) to obtain blood cell-free serum fraction. Two types of solutions were prepared: (1) CAM blood and (2) CAM blood serum (hereinafter, serum). Fifty microliter of CAM blood or serum were mixed with 20 μl Ru(Phen) solutions (0.5 and 0.01 mg/ml) and placed in 150-μl plastic containers. These samples were stabilized during 1 h in the dark and installed in a chamber (0.28 l) with gas, temperature, and humidity controlled. The chamber is integrated in the lifetime measurement setup (Fig. 2). The fiber of the time-resolved spectrometer was positioned perpendicularly ~2 mm above the solutions. This distance was defined in such a way that the luminescence was detected from a 1-mm^2 surface (Fig. 2). Ru(Phen) solutions were subjected to gas flow during 15 min with defined oxygen concentration (0, 5, 10, 15, and 21% of O_2 in N_2 M/M) prior to measurement. The gas flow (~3 l/h) and humidity (100%) were controlled and measured with the gas mixer (The BRICK). Temperature was stabilized at 30°C with a thermostabilizer (The CUBE; Life Imaging Services GmbH, Switzerland). The temperature was kept the same as the CAM temperature during *in vivo* pO_2 measurements. The reciprocal values of Ru(Phen) luminescence lifetimes were plotted for different pO_2. This approach enables us to perform a linear fit of the data since the lifetime and pO_2 are governed by the Stern-Volmer relation [Eq. (3)]:

$$\tau_0/\tau = 1 + \tau_0 k_q(pO_2), \tag{3}$$

where τ and τ_0 are the Ru(Phen) luminescence lifetimes in the presence and absence of oxygen, respectively. k_q is the bimolecular quenching constant and (pO_2) is oxygen partial pressure. Eight lifetime measurements were averaged to generate one point in Fig. 6.

The same protocol and approach were applied to obtain the comparative Stern-Volmer relations by using standard oxygen sensor Oxyphor R0 (0.5 mg/ml PdTCPP at pH 7.4) in the CAM blood and serum [V (PdTCPP): V(blood/serum) = 20 μl : 50 μl).

2.9.2 In vivo measurements

In vivo measurements of Ru(Phen) luminescence lifetimes were performed at EDD 11 and 12. An egg was placed into a chamber (0.28 l) with gas, temperature, and humidity controlled, integrated in the lifetime measurement setup (Fig. 2). Twenty microliters of Ru(Phen) solution corresponding to a dose of 1 mg/kg were injected into a vein. The fiber of the time-resolved spectrometer was positioned perpendicularly ~2 mm above the membrane. Two main areas of interest were defined: (1) intravascular compartments (100 μm < vessels) and (2) extravascular compartments (vessels < 100 μm) (see Fig. 2). A delay of 10 min was observed before all measurements, while flushing

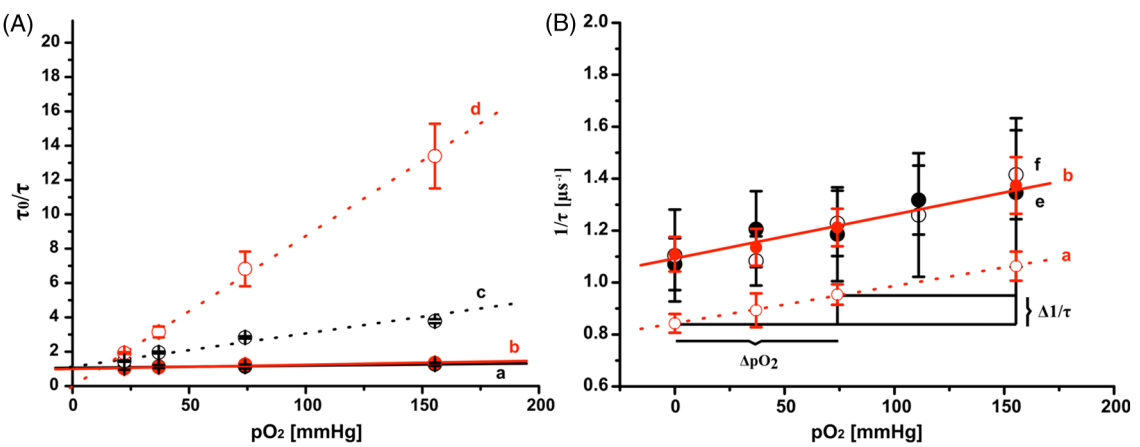

Fig. 6 (A) pO_2 resolution of [(a) and (b)] Ru(phen) or [(c) and (d)] PdTCPP represented by the ratio of the luminescence lifetimes measured in the absence (τ_0) and presence (τ) of oxygen for different pO_2 values of a gas mixture in biological liquids: (a) RuPhen in the serum, (b) Ru(Phen) in the blood ($p = 0.6$, serum/blood), (c) PdTCPP in the serum, and (d) PdTCPP in the blood (*$p = 0.03$, blood/serum). (two repetitions). (B) Stern-Volmer characteristics of Ru(Phen) reciprocal luminescence lifetimes measured *in vivo* as a function of the environmental pO_2 (f) in the intravascular space and (e) in the extravascular space, and the pO_2 calibration curves obtained (a) in the blood and (b) in the serum. The significantly measured values of differences ΔpO_2 and $\Delta 1/\tau$ in our condition are displayed by black lines with arrows.

the gas chamber with a flux of ~3 l/h, after each change of O_2 concentration. Oxygen concentrations of 0, 5, 10, 15, and 21% O_2 in N_2 M/M were applied. During the measurements, the temperature of CAM was measured with noncontact infrared thermometer (Raytek a Fluke Company, Santa Cruz, California) positioned 1 cm above the CAM and covering a 25-mm^2 surface. The mean value of CAM temperatures was 30°C. Ru(Phen) excitation and luminescence were performed on a 1-mm^2 surface. The 470-nm laser fluence applied for one measurement did not exceed 120 mJ/cm^2. The data were processed and analyzed as mentioned above by fitting the measurements with the mono-exponential function [Eq. (2)]. Reciprocal lifetimes of Ru(Phen) in intra/extravascular compartments were inserted in the Stern-Volmer relation [Eq. (3)]. Six eggs were investigated per set of experimental conditions.

2.10 *Biodistribution of Ru(Phen) in Tumor-CAM Model*

Tumors were grafted on the CAM as described above. Twenty microliters of a solution containing a Ru(Phen) dose corresponding to 10 mg/kg were injected intravenously to tumor-bearing CAMs. Ru(Phen) angiography was recorded 10 min after injection. Black ink was also used to screen the tissue autofluorescence, as described above. White light image of the tumor-CAM model was obtained using a standard camera (Nikon).

2.11 *Measurement of Ru(Phen) Luminescence Lifetime in Tumor Model*

Twenty microliters of a solution containing a Ru(Phen) dose corresponding to 1 mg/kg were injected intravenously into a CAM 10 min prior to luminescence lifetime measurement. All eggs were kept at 37°C in the dark until the measurement. Two main regions of interest were defined: (1) a region corresponding to a tumor inoculation and (2) a region with the physiological CAM vessels (not in a tumor). Ru(Phen) luminescence lifetime measurements were performed in standard room conditions (25°C and ambient pO_2) on seven eggs according to the procedure described above. The temperature of CAM did not drop under 30°C.

Statistical significance was evaluated with the Student's t test using the Origin software with significance level $p = 0.05$.

3 Results

3.1 *Ru(Phen) Pharmacokinetics and Biodistribution in CAM*

Typical luminescence angiographies obtained after intravenous injection of Ru(Phen) solutions (dose of 10 mg/kg) for vessels presenting diameters of ~70 and 450 μm (see white arrows) are given in Fig. 7.

Uptake of Ru(Phen) by the walls appears in the profile plot as two intense maxima [Fig. 7(c)]. Ru(Phen) intravascular luminescence intensity was high compared to the extravascular space in both small and large vessels shortly (20 s) after injection, suggesting that Ru(Phen) is inside the vessel and fully distributed throughout the entire vascular system already 1 min after the injection [Fig. 7(b)]. Profile plot of the vessel section shows increased fluorescence intensity in the area corresponding to the intravascular space during the initial minute after injection, thus confirming homogeneous intravascular distribution [Fig. 7(b)]. While the profile plot of the vessel section showed higher intensities in the extravascular space compared to intravascular space in Fig. 7(a), this observation is reversed in Fig. 7(b): intravascular intensity of Ru(Phen) was more than 100 times higher than extravascular intensity. Interestingly, luminescence angiography of Ru(Phen) performed 10 min after injection showed a high accumulation of Ru(Phen) in the walls of the large vessels and initial accumulation in the extravascular space [Fig. 7(c)]. It should be noted that the intensity ratio between intracellular and extracellular spaces rapidly decreased (see Fig. 4). This indicates that Ru(Phen) leaks out of

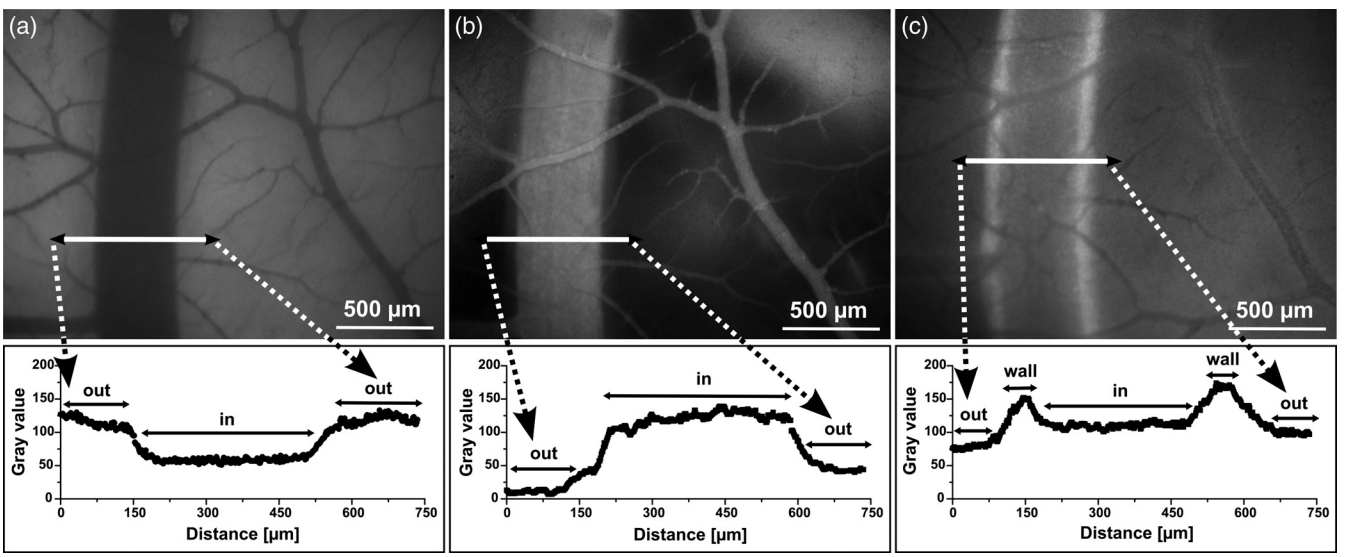

Fig. 7 Biodistribution of Ru(Phen) (10 mg/kg, intravenous injection) within large and small CAM blood vessels as well as in the extravascular space: (a) typical CAM picture prior the Ru(Phen) and black ink administration, (b) 1 min after Ru(Phen) injection, (c) 10 min after Ru(Phen) injection. Profile plots represent local intensities of Ru(Phen) throughout the section of the blood vessel marked with white arrow.

the vessels. Therefore, the luminescence pharmacokinetics of Ru(Phen) was evaluated within 10 min. Normalized photographic contrast C_{phot} for intravascular space and vessel walls determined from Eq. (1) at different times following the injection is presented in Fig. 4. The intravascular C_{phot} rapidly decreases to 50% of its initial value, reaching a plateau at 0.55 after 5 min (Fig. 4). On the other hand, C_{phot} in the wall increases to the plateau at 0.8, which represents 80% of the initial value of intravascular C_{phot}. As C_{phot} represents intravascular concentration of Ru(Phen), it means that ~20% of initial concentration is lost.

3.2 *Acute Dark Toxicity of Ru(Phen)*

Since higher doses will lead to a better signal/noise ratio in compartments producing a low luminescence, such as the extravascular space, we have assessed the dark toxicity of Ru(Phen). All eggs treated with Ru(Phen) doses ranging between 1 and 200 mg/kg survived up to 72 h after injection. In addition, no vascular damage, such as vessel occlusions, has been observed (data not shown).

3.3 *Ru(Phen) Phototoxicity Assessment*

Although Ru(Phen)'s dark toxicity seems to be limited, its phototoxicity must be assessed to determine the nature of the photodamage and tissue perturbation induced during pO_2 measurements. Like other luminescent oxygen-sensitive probes, Ru(Phen) is likely to be a photo-sensitizing molecule. The effect on the CAM vascular plexus of Ru(Phen) doses ranging between 1 and 20 mg/kg excited by light with the fluence ranging between 1 and 10 J/cm^2 is given in Fig. 5. Considering the Ru(Phen) biodistribution described above, two DLIs have been considered, i.e., 1 and 10 min. FITC-dextran angiographies performed 24 h after illumination showed that Ru(Phen) doses and fluence <1 mg/kg and 10 J/cm^2, respectively, did not induce any visible vascular damage [Figs. 5(b), 5(e), and 5(g)]. These values were defined as the phototoxic threshold. A maximal index of vascular damage of ~3 (see Sec. 2 for details on the vascular damage scale) was obtained with the 20-mg/kg Ru(Phen) dose and the fluence at 10 J/cm^2 [Fig. 5(f)]. Interestingly, no significant difference was observed between the two DLIs (1 and 10 min after Ru(Phen) injection) [Fig. 5(g)].

3.4 *pO_2 Measurements Based on Ru(Phen) Luminescence Lifetime*

3.4.1 *Measurements in solutions*

The ratio τ_0/τ was plotted as a function of pO_2. Figure 6(A) shows Ru(Phen) τ_0/τ dependences in presence of (a) serum and (b) CAM blood. In both cases, a linear correlation was found on the entire pO_2 range (from 0 to 155.4 mm Hg). The parameters of the Stern-Volmer equation [(a) $1/\tau = 1.093 + 0.00169$ (pO_2) and (b) $1/\tau = 0.843 + 0.00143$ (pO_2)] were derived in Table 1 and compared with those obtained for standard oxygen sensor PdTCPP [Table 1 and Fig. 6(A)]. While Ru(Phen) luminescence lifetime in the absence of oxygen is 1.20 ± 0.11 μs in the serum fraction, we have measured a value 1.02 ± 0.05 μs in the presence of CAM blood. For PdTCPP, we observed 88 ± 11 μs in the serum and 142 ± 26 μs in the blood. From the Stern-Volmer relations in Fig. 6, we determined τ_0/τ_{Air} ratio between luminescence lifetime in the absence of oxygen and in atmospheric pO_2. We found $\tau_0/\tau_{Air} = 1.26$ for Ru(Phen) in the serum and in the presence of blood $\tau_0/\tau_{Air} = 1.25$. In the case of PdTCPP, values of $\tau_0/\tau_{Air} = 5.45$ in the serum and $\tau_0/\tau_{Air} = 17.46$ were calculated. Composition of the solution affects not only luminescence lifetimes but also quenching constants (k_q): the presence of blood cells in the solutions increases k_q values of both oxygen-sensitive molecules: Ru(Phen) from 1.43×10^{-3} to 1.69×10^{-3} mm Hg^{-1} μs^{-1} and PdTCPP from 0.26×10^{-3} to 0.56×10^{-3} mm Hg^{-1} μs^{-1} (Table 1).

3.4.2 *In vivo measurements*

The variations of Ru(Phen) luminescence lifetimes measured in CAM were dependent on the variation of external pO_2 in a range from 0 up to 155.4 mm Hg. The reciprocal lifetimes of Ru(Phen) localized intra- and extravascularly were plotted in Fig. 6(B). Significantly different values ($^{**}p < 0.001$) were reached in the ambient pO_2: 1.34 ± 0.28 μs^{-1} (intravascular) and 1.41 ± 0.17 μs^{-1} (extravascular), and in the absence of oxygen: 1.07 ± 0.09 μs^{-1} (intravascular) and 1.10 ± 0.17 μs^{-1} (extravascular). We found a similar Stern-Volmer relation of Ru(Phen) lifetimes in both compartments [Fig. 6(B)]. Despite higher standard deviations compared to the physiological solutions (serum/blood), these pO_2 dependences are still linear and almost identical with Ru(Phen) lifetimes obtained in the presence of CAM blood [Fig. 6(B)].

Table 1 Stern-Volmer parameters of dichlorotris(1,10-phenanthroline)-ruthenium(II) hydrate [Ru(Phen)] and Pd-meso-tetra(4-carboxyphenyl)porphyrin (PdTCPP) in biological liquids: (1) blood and (2) serum fraction. Parameters were derived from the linear oxygen dependence of Ru(Phen)/PdTCPP luminescence lifetimes presented in Fig. 6(A). τ_0 represents luminescence lifetime in the absence of oxygen, τ_{Air} is luminescence lifetime in ambient oxygen partial pressure (155.4 mm Hg), and k_q is a bimolecular quenching constant.

Stern-Volmer parameters	Derived τ_0 (μs)	τ_0/τ_{Air}	k_q (mm Hg^{-1} μs^{-1})	$\tau_0 k_q$ (mm Hg^{-1})
PdTCPP in extracted CAM blood	189	17.46	0.56×10^{-3}	105.8×10^{-3}
PdTCPP in CAM blood serum fraction	112	5.45[a]	0.26×10^{-3}[a]	29.1×10^{-3}
Ru(Phen) in extracted CAM blood	0.91	1.25	1.69×10^{-3}	1.5×10^{-3}
Ru(Phen) in CAM blood serum fraction	1.18	1.26	1.43×10^{-3}	1.6×10^{-3}

Note: CAM, chorioallantoic membrane; $p = 0.6$ [Ru(Phen) blood/serum].
[a]$p = 0.03$ (PdTCPP blood/serum).

3.5 *Measurement of Ru(Phen) Luminescence Lifetime in Tumor Model*

An illustrative application of this pO_2 measurement approach in a tumor model is presented in Fig. 3. Ten minutes after Ru(Phen) intravenous injection, the uptake of Ru(Phen) by the tumor model was sufficient for luminescence imaging [Fig. 3(a)]. Ru(Phen) luminescence lifetimes were measured noninvasively at the surfaces of seven small (2 to 3 mm in diameter) tumors grafted on CAM [see arrow in Fig. 3(d)]. Ru(Phen) luminescence decays were obtained from the physiological (not dedicated to tumor) CAM vessels and from the tumoral vessels [Fig. 3(c)]. While the reciprocal lifetimes in the physiological CAM vessels are comparable to those reported in Fig. 6(B) for eggs in ambient pO_2 ($1.45 \pm 0.14\ \mu s^{-1}$, the measurements performed on the tumor vessels were much more heterogeneous and indicated significantly shorter reciprocal lifetimes [$0.97 \pm 0.14\ \mu s^{-1}$, see Fig. 3(c)].

4 Discussion

The biodistribution and further accumulation of a drug in a tissue depends on its hydrophobic or hydrophilic properties, as well as its affinity for biomacromolecular structures (e.g., subcellular organelles, membranes, proteins, etc.). Hydrophilic compounds, such as fluorescein, usually have a very fast body clearance, mainly via renal excretion.[43] In many cases, this fast clearance is advantageous because it limits the drug toxicity. A rapid decrease of Ru(Phen) concentration in the bloodstream was observed within 10 min after intravenous injection in rodents.[31] Ru(Phen) was excreted in urine and no trace thereof was found in the nervous system.[31] This is one of the reasons Ru (Phen) was, in an experiment to visualize pO_2 in hepatic tissues, continuously infused in rats during intravital microscopy to reach a constant Ru(Phen) concentration in plasma.[33]

We have also observed a rapid decrease in Ru(Phen) intravascular intensity during the first minutes after intravenous injection (Fig. 7). This can be due to a fast leakage of the molecules out of the vessels (faster leakage from small vessels than from larger vessels). For the sake of this study, we proposed to talk about intravascular measurements when the fiber was probing an area containing vessels with diameters $>100\ \mu m$, whereas the term extravascular was used when this area contained smaller vessels only. However, this clearance was not similar to that of a typical hydrophilic compound. Indeed, the temporal evolution of the photographic contrast after intravenous injection of hydrophilic Ru(Phen) in the CAM is very similar to that of the more lipophilic benzoporphyrin derivative monoacid ring A (BPD-MA),[37] whereas we would have expected a behavior similar to that of water-soluble fluorescein.[37] Additionally, we found an increasing Ru(Phen) accumulation in the walls of large (diameter $> 100\ \mu m$) vessels (Fig. 7). These biodistribution and pharmacokinetics observations suggest that the pO_2 can be realistically measured in three compartments (bloodstream, vessel wall, extravascular space) with a time-resolved microspectrophotometric setup and at appropriate times after injection of appropriate Ru (Phen) doses. It is interesting to note that this sets the Ru (Phen)-mediated measurement of pO_2 apart from more standard, noninvasive techniques, such as pulse oxymetry, which can only measure intravascular changes of oxygen.

We were not able to distinguish subcellular localization of Ru (Phen) *in vivo*, but cell culture studies showed Ru(Phen)'s possible localization in the endocytic vesicles in the cytoplasm and in the membrane.[36] It was reported that even if Ru(Phen) is transported inside the cells via endocytic pathway, the content concentration of Ru(Phen) in the extracellular space remains higher than in the intracellular space.[36] Thus, any energy transfer between excited Ru(Phen) and oxygen may occur mainly near cellular membranes.

We demonstrated that Ru(Phen) has limited dark toxicity and phototoxicity. This sets it apart from a number of other molecules of relevance to photodynamic therapy (PDT) (porfimer sodium, verteporfin, and purpurins), which display high phototoxicity, and can cause vessel closure. Several studies report alterations of the vascular endothelium during irradiation of tissues *in vivo*, photosensitized with them.[12,44–47] At short DLIs, *in vivo*[12,44,48] endothelial dysfunction and blood flow stasis followed by vessel occlusion appear to be their predominant mechanisms of damage. Moreover, a direct correlation between the vascular changes and the amount of photosensitizer in circulation during photodynamic therapy has been suggested.[44]

This also holds true for commonly used oxygen sensor PdTCPP bound to albumin, whose intravascular concentration remains nearly constant over several hours and has been shown to be highly phototoxic.[12] While PdTCPP-albumin complex is kept inside the vessels, Ru(Phen) weakly binds with proteins[49] and rapidly leaks out of the vessels to extravascular space (Fig. 7). Mechanisms of vascular damage induced by Ru (Phen) will probably be governed by pathways other than those of PdTCPP.

Photodamage is the result of the interaction of photoactivated molecules with oxygen due to singlet oxygen production. In contrast to approved photosensitizers used in photodynamic therapy, e.g., verteporfin [BPD-MA, quantum yield of singlet oxygen production Φ_Δ in methanol is 0.78 (Ref. 50)], the quantum yield of singlet oxygen production (Φ_Δ) of Ru(Phen) is very low [Φ_Δ in D_2O is 0.24 (Ref. 16)], but higher than, e.g., fluorescein used for photodiagnosis in ophthalmology [Φ_Δ in H_2O is 0.03 (Ref. 16)]. We found that we need only 0.2 mg/kg of BPD-MA,[51] but up to 20 mg/kg of Ru(Phen) to reach photodamage with vascular index 3 after application of a fluence of 10 J/cm^2.

While photodynamic therapy requires enough cellular damage to kill a cell, pO_2 measurements need to avoid this outcome. Highly sensitive detection systems, low Ru(Phen) concentration (1 mg/kg) with high emission quantum yield, and fluence two orders of magnitude lower than phototoxic threshold (120 mJ/cm^2) are an excellent combination for noninvasive pO_2 assessment.

We carried out a comparative study of oxygen sensitivity of Ru(Phen) and PdTCPP, two water-soluble molecules, in a different microenvironment related to *in vivo* conditions: a blood and a serum sample. In these conditions, intact blood cells are present in the blood sample. The serum cell-free fraction consisted of a natural mixture of CAM serum proteins. Each modification of the environment can lead to modifications of the oxygen sensitivity of probes. PdTCPP is a highly pH-sensitive probe and well dissolved at alkaline pH. Similar to other porphyrin-based complexes, its primary subcellular targets are mitochondria.[52] Thus, it is not surprising that PdTCPP's k_q value is higher in CAM blood samples than in the serum fraction, where it can be dissolved in red blood cell mitochondria. Ru(Phen) in contrast to PdTCPP is relatively pH independent,[53] and k_q values of Ru(Phen) in both microenvironments are not significantly different (Table 1).

Both PdTCPP and Ru(Phen) luminescence lifetimes showed a linear Stern-Volmer pO_2 dependence in CAM blood and serum solutions (Fig. 6). However, we have measured significantly shorter τ_0 of Ru(Phen) in the blood samples than in serum. This is a surprising result, as we would have expected to measure the same Ru(Phen) luminescence lifetime in both microenvironments. A possible explanation could be that measurements were performed starting at physiological temperature and then going down to 30°C as the eggs stayed outside the incubator and cooled somewhat. Such a temperature does not suppress metabolism in the blood cells. In conditions of normoxia (ambient pO_2), enzymatic process of glycolysis is inhibited by the presence of oxygen, and pyruvate in mitochondria is oxidized to CO_2 and H_2O.[54] When pO_2 decreases, hypoxia induces acceleration of glycolysis.[55] In this process, glucose is converted to lactate.[55] It was reported that erythrocytes in the hypoxic condition accelerate glucose consumption.[56] Production of lactic acid leads to pH drop. As it is known, erythrocytes deliver molecular oxygen to tissues through allosteric regulation of hemoglobin;[57] the oxygen affinity of hemoglobin decreases with lowering pH, which results in the release of oxygen from oxyhemoglobin.[58] This residual oxygen can be further involved in the luminescence quenching process and induce shortening of Ru(Phen) lifetimes in the blood samples. Thus, it could be envisioned that Ru(Phen) could be used to monitor not only pO_2, but also glycolysis. Additionally, it was recently reported that a combination of Ru(Phen) and a glucose oxidase enzyme was used to monitor glucose *in vitro* in the macrophage[35] and when immobilized in polymeric bilayers as a component of glucose biosensors.[59,60]

Oxygen-dependence of Ru[Phen] luminescence lifetimes in solutions was previously reported whether alone or in a combination with other sensors.[20–22] However, there are only few studies about Ru(Phen) oxygen sensitivity *in vivo*,[33,61,62] and none of them focuses on luminescence lifetimes. The vasculature of CAM creates the main access for gas exchange. Using Ru (Phen) luminescence lifetime measurements, we demonstrated that any fluctuation of external pO_2 rapidly influences intravascular pO_2 [see Fig. 6(B)]. Ru(Phen) luminescence lifetimes measured in the intravascular and extravascular space were governed by Stern-Volmer oxygen dependences and were not significantly different from each other [Fig. 6(B)]. It should also be noted that during our experiment, we had to change the measurement location on CAM (a heterogenous membrane) between each measurement, which adds real CAM-intrinsic fluctuations to the pO_2 fluctuations. Measurements performed in one location only show much fewer variations (data not shown). Wilson et al. observed similar relationship of pO_2 in the interstitial space and in the blood plasma on a mouse model using phosphorescence of oxyphors G3 and G2, respectively.[63] CAM plexus is well perfused and contains high numbers of erythrocytes for oxygen transport. Thus, Stern-Volmer relations obtained *in vivo* are closely related to calibration preformed in the blood sample [Fig. 6(B)].

Finally, we have illustrated the advantage of this pO_2 measurement approach compared to invasive probes. It should be noted that this advantage is particularly striking when superficial measurements are carried out, i.e., to a depth of several hundred microns. The limited penetration of Ru(Phen) excitation light prevents pO_2 measurements deeper in the tissues.[42] Nevertheless, interstitial measurements of Ru(Phen) luminescence can also be performed with a fiber that can potentially be much thinner than that of the standard systems,[10,11] thus reducing the tissue damages. In our CAM-tumor model, tumoral tissues are less perfused than the physiological tissues.[64] As pO_2 in hypoxic tumor decreases from the surface to the core,[65] our measurements at the surface of the CAM-tumor model can be affected by ambient pO_2. In spite of this, significantly shorter reciprocal lifetimes were found in the tumor compared to physiological tissue. The pO_2 fluctuations as a function of distance from the tumoral tissue can be precisely defined using luminescence lifetime imaging. In general, imaging approaches require high luminescent drug concentrations to decrease signal/noise ratio and to acquire a good-resolution image. Because Ru (Phen) possesses enough luminescence intensity for lifetime detection at low concentrations, it is a very promising oxygen probe suitable for lifetime imaging. Furthermore, low phototoxicity of Ru(Phen) offers a possibility to coadminister it in combination with photodynamic agents. Photodynamic therapy can be performed only in oxygenated tissues.[66] In the absence of oxygen, this therapy is not applicable. Thus, determination of tissue oxygenation with Ru(Phen) can indicate in which tissues PDT will be successful.

5 Conclusions

In this study, we have evidenced Ru(Phen)'s intra/extravascular biodistribution, fast pharmacokinetics, and very low *in vivo* phototoxicity. Noninvasive, highly sensitive, optical, time-domain-based luminescence lifetime measurement technique was demonstrated to easily detect Ru(Phen) luminescence lifetimes in different microenvironments. Furthermore, we have demonstrated that Ru(Phen)'s luminescence lifetimes in various microenvironments present linear Stern-Volmer oxygen dependences not only in the biological liquids (CAM blood and serum) but also *in vivo* in the intra/extravascular space of CAM. Reliable and easy pO_2 prediction was illustrated in CAM tumors with this approach.

Acknowledgments

The authors thank Debora Bonvin and Andrea Weiss for help in chorioallantoic membrane tumor models preparation. This work was supported with Sciex (Scientific exchange programme NMS-CH) Project No. 10.142, Swiss National Science Foundation Project No. 205320-130518, Project No. 205320_147141, and Project No. CR32I3_150271. This work was also supported by the Dr. Jacobi Trust and the Project CELIM 316310 funded by EU 7FP.

References

1. X.-D. Wang and O. S. Wolfbeis, "Optical methods for sensing and imaging oxygen: materials, spectroscopies and applications," *Chem. Soc. Rev.* **43**(10), 3666 (2014).
2. R. I. Dmitriev and D. B. Papkovsky, "Optical probes and techniques for O_2 measurement in live cells and tissue," *Cell. Mol. Life Sci.* **69**(12), 2025–2039 (2012).
3. J. B. West, *Respiratory Physiology—The Essentials*, Blackwell Scientific, Oxford (1974).
4. P. Vaupel, "Tumor microenvironmental physiology and its implications for radiation oncology," *Semin. Radiat. Oncol.* **14**(3), 198–206 (2004).
5. P. Howard-Flanders and O. C. Scott, "Tissue oxygen tension and radiotherapy. A review and bibliography based on a conference in Burlington, Vermont, August 1958," *Radiology* **74**, 956–963 (1960).
6. M. Hockel and P. Vaupel, "Tumor hypoxia: definitions and current clinical, biologic, and molecular aspects," *J. Natl. Cancer Inst.* **93**(4), 266–276 (2001).

7. C. Menon and D. L. Fraker, "Tumor oxygenation status as a prognostic marker," *Cancer Lett.* **221**(2), 225–235 (2005).
8. H. G. Hou et al., "Repeated tumor pO(2) measurements by multi-site EPR oximetry as a prognostic marker for enhanced therapeutic efficacy of fractionated radiotherapy," *Radiother. Oncol.* **91**(1), 126–131 (2009).
9. E. G. Mik et al., "Mitochondrial PO2 measured by delayed fluorescence of endogenous protoporphyrin IX," *Nat. Methods* **3**(11), 939–945 (2006).
10. D. R. Collingridge et al., "Measurement of tumor oxygenation: a comparison between polarographic needle electrodes and a time-resolved luminescence-based optical sensor," *Radiat. Res.* **147**(3), 329–334 (1997).
11. J. R. Griffiths and S. P. Robinson, "The OxyLite: a fibre-optic oxygen sensor," *Br. J. Radiol.* **72**(859), 627–630 (1999).
12. T. K. Stepinac et al., "Light-induced retinal vascular damage by Pd-porphyrin luminescent oxygen probes," *Invest. Ophthalmol. Vis. Sci.* **46**(3), 956–966 (2005).
13. P. Nowak-Sliwinska et al., "Study of the pO2-sensitivity of the dendrimeric and free forms of Pd-meso-tetra(4-carboxyphenyl)porphyrin, incorporated or not in chitosan-based nanoparticles," *Chimia (Aarau)* **65**(9), 691–695 (2011).
14. F. Piffaretti et al., "Real-time, in vivo measurement of tissular pO2 through the delayed fluorescence of endogenous protoporphyrin IX during photodynamic therapy," *J. Biomed. Opt.* **17**(11), 115007 (2012).
15. P. Gbur et al., "Time-resolved luminescence and singlet oxygen formation after illumination of the hypericin-low-density lipoprotein complex," *Photochem. Photobiol.* **85**(3), 816–823 (2009).
16. H. Sterenborg et al., "Phosphorescence-fluorescence ratio imaging for monitoring the oxygen status during photodynamic therapy," *Opt. Express* **12**(9), 1873–1878 (2004).
17. M. C. DeRosa and R. J. Crutchley, "Photosensitized singlet oxygen and its applications," *Coord. Chem. Rev.* **233**, 351–371 (2002).
18. J. N. Demas and B. A. Degraff, "Applications of highly luminescent transition-metal complexes in polymer systems," *Macromol. Symp.* **59**(1), 35–51 (1992).
19. W. Y. Xu, J. N. Demas, and B. A. Degraff, "Highly luminescent transition-metal complexes as sensors," *Proc. SPIE* **2131**, 417–425 (1994).
20. D. P. O'Neal et al., "Oxygen sensor based on the fluorescence quenching of a ruthenium complex immobilized in a biocompatible poly(ethylene glycol) hydrogel," *IEEE Sens. J.* **4**(6), 728–734 (2004).
21. C. Baleizao et al., "Dual fluorescence sensor for trace oxygen and temperature with unmatched range and sensitivity," *Anal. Chem.* **80**(16), 6449–6457 (2008).
22. S. M. Grist, L. Chrostowski, and K. C. Cheung, "Optical oxygen sensors for applications in microfluidic cell culture," *Sensors (Basel)* **10**(10), 9286–9316 (2010).
23. H. Kobayashi and Y. Kaizu, "Photodynamics and electronic-structures of metal-complexes," *Coord. Chem. Rev.* **64**(May), 53–64 (1985).
24. J. N. Demas and G. A. Crosby, "On the multiplicity of emitting state of ruthenium(2) complexes," *J. Mol. Spectrosc.* **26**(1), 72–77 (1968).
25. Z. Rosenzweig and R. Kopelman, "Analytical properties of miniaturized oxygen and glucose fiber optic sensors," *Sens. Actuators B Chem.* **36**(1–3), 475–483 (1996).
26. F. P. Dwyer et al., "Biological activity of complex ions," *Nature* **170** (4318), 190–191 (1952).
27. F. P. Dwyer et al., "Inhibition of Landschutz Ascites tumour growth by metal chelates derived from 3,4,7,8-tetramethyl-1,10-phenanthroline," *Br. J. Cancer* **19**(1), 195–199 (1965).
28. D. O. White et al., "Actions of metal chelates of substituted 1,10-phenanthrolines on viruses and cells. 1. Inactivation of viruses," *Aust. J. Exp. Biol. Med.* **41**(5), 517–526 (1963).
29. D. O. White, A. Shulman, and A. W. Harris, "Actions of metal chelates of substituted 1,10-phenanthrolines on viruses and cells. 2. Inhibition of viral multiplication," *Aust. J. Exp. Biol. Med.* **41**(5), 527–537 (1963).
30. D. O. White et al., "Actions of metal chelates of substituted 1,10-phenanthrolines on viruses and cells. 3. Actions on cultured cells," *Aust. J. Exp. Biol. Med.* **47**(1), 81–89 (1969).
31. J. H. Koch et al., "The metabolic fate of tris-1, 10-phenanthroline 106ruthenium (II) perchlorate, a compound with anticholinesterase and curare-like activity," *Aust. J. Biol. Sci.* **10**(3), 342–350 (1957).
32. A. Yadav et al., "Regression of lung cancer by hypoxia-sensitizing ruthenium polypyridyl complexes," *Mol. Cancer Ther.* **12**(5), 643–653 (2013).
33. M. Paxian et al., "High-resolution visualization of oxygen distribution in the liver in vivo," *Am. J. Physiol. Gastrointest. Liver Physiol.* **286**(1), G37–44 (2004).
34. T. N. Tan, R. H. Weston, and J. P. Hogan, "Use of 103Ru-labelled tris (1, 10-phenanthroline) ruthenium (II) chloride as a marker in digestion studies with sheep," *Int. J. Appl. Radiat. Isot.* **22**(5), 301–308 (1971).
35. J. K. Asiedu et al., "Development of a digital fluorescence sensing technique to monitor the response of macrophages to external hypoxia," *J. Biomed. Opt.* **6**(2), 116–121 (2001).
36. J. W. Dobrucki, "Interaction of oxygen-sensitive luminescent probes Ru(phen)(3)(2+) and Ru(bipy)(3)(2+) with animal and plant cells in vitro—mechanism of phototoxicity and conditions for non-invasive oxygen measurements," *J. Photochem. Photobiol. B* **65**(2–3), 136–144 (2001).
37. N. Lange et al., "A new drug-screening procedure for photosensitizing agents used in photodynamic therapy for CNV," *Invest. Ophthalmol. Vis. Sci.* **42**(1), 38–46 (2001).
38. B. Pegaz et al., "Photothrombic activity of m-THPC-loaded liposomal formulations: pre-clinical assessment on chick chorioallantoic membrane model," *Eur. J. Pharm. Sci.* **28**(1–2), 134–140 (2006).
39. P. Nowak-Sliwinska et al., "Processing of fluorescence angiograms for the quantification of vascular effects induced by anti-angiogenic agents in the CAM model," *Microvasc. Res.* **79**(1), 21–28 (2010).
40. F. Piffaretti et al., "Optical fiber-based setup for in vivo measurement of the delayed fluorescence lifetime of oxygen sensors," *J. Biomed. Opt.* **16**(3), 037005 (2011).
41. Y. Adar et al., "Imidazoacridinone-dependent lysosomal photodestruction: a pharmacological Trojan horse approach to eradicate multidrug-resistant cancers," *Cell Death Dis.* **3**(4), e293 (2012).
42. G. Wagnieres et al., "An optical phantom with tissue-like properties in the visible for use in PDT and fluorescence spectroscopy," *Phys. Med. Biol.* **42**(7), 1415–1426 (1997).
43. "Material Safety Data Sheet FLUORESCEIN Novartis 500 mg/5 mL (fluorescein sodium)," http://www.novartis.com.au/products/healthcare-professionals.shtml (21 June 2014).
44. V. H. Fingar, "Vascular effects of photodynamic therapy," *J. Clin. Laser Med. Surg.* **14**(5), 323–328 (1996).
45. B. Krammer, "Vascular effects of photodynamic therapy," *Anticancer Res.* **21**(6B), 4271–4277 (2001).
46. P. Fungaloi et al., "Photochemically modulated endothelial cell thrombogenicity via the thrombomodulin-tissue factor pathways," *Photochem. Photobiol.* **78**(5), 475–480 (2003).
47. F. Adili et al., "Photodynamic therapy mediated induction of accelerated re-endothelialisation following injury to the arterial wall: implications for the prevention of postinterventional restenosis," *Eur. J. Vasc. Endovasc. Surg.* **24**(2), 166–175 (2002).
48. U. Schmidt-Erfurth and T. Hasan, "Mechanisms of action of photodynamic therapy with verteporfin for the treatment of age-related macular degeneration," *Surv. Ophthalmol.* **45**(3), 195–214 (2000).
49. L. Luzuriaga and M. F. Cerda, "Analysis of the interaction between [Ru (phenanthroline)3]2+ and bovine serum albumin," *Adv. Biol. Chem.* **2**, 262–267 (2012).
50. B. Aveline, T. Hasan, and R. W. Redmond, "Photophysical and photosensitizing properties of benzoporphyrin derivative monoacid ring A (BPD-MA)," *Photochem. Photobiol.* **59**(3), 328–335 (1994).
51. E. Debefve et al., "Video monitoring of neovessel occlusion induced by photodynamic therapy with verteporfin (Visudyne (R)), in the CAM model," *Angiogenesis* **11**(3), 235–243 (2008).
52. Y. Kabe et al., "Porphyrin accumulation in mitochondria is mediated by 2-oxoglutarate carrier," *J. Biol. Chem.* **281**(42), 31729–31735 (2006).
53. I. Kasik et al., "Fiber-optic pH detection in small volumes of biosamples," *Anal. Bioanal. Chem.* **398**(5), 1883–1889 (2010).
54. E. Racker, "History of the Pasteur effect and its pathobiology," *Mol. Cell. Biochem.* **5**(1–2), 17–23 (1974).
55. R. A. Gatenby and R. J. Gillies, "Why do cancers have high aerobic glycolysis?," *Nat. Rev. Cancer* **4**(11), 891–899 (2004).
56. J. R. Murphy, "Erythrocyte metabolism. II. Glucose metabolism and pathways," *J. Lab Clin. Med.* **55**, 286–302 (1960).

57. J. M. Berg, J. L. Tymoczko, and L. Stryer, Eds., "Hemoglobin transports oxygen efficiently by binding oxygen cooperatively," Section 10.2 in *Biochemistry*, 5th ed., W. H. Freeman, New York (2002).
58. A. Kinoshita et al., "Roles of hemoglobin allostery in hypoxia-induced metabolic alterations in erythrocytes—simulation and its verification by metabolome analysis," *J. Biol. Chem.* **282**(14), 10731–10741 (2007).
59. L. Li and D. R. Walt, "Dual-analyte fiberoptic sensor for the simultaneous and continuous measurement of glucose and oxygen," *Anal. Chem.* **67**(20), 3746–3752 (1995).
60. M. C. Morenobondi et al., "Oxygen optrode for use in a fiber-optic glucose biosensor," *Anal. Chem.* **62**(21), 2377–2380 (1990).
61. V. M. Victor et al., "Regulation of oxygen distribution in tissues by endothelial nitric oxide," *Circ. Res.* **104**(10), 1178–1183 (2009).
62. T. Itoh et al., "In vivo visualization of oxygen transport in microvascular network," *Am. J. Physiol.* **267**(5 Pt 2), H2068–2078 (1994).
63. D. F. Wilson et al., "Oxygen pressures in the interstitial space and their relationship to those in the blood plasma in resting skeletal muscle," *J. Appl. Physiol.* **101**(6), 1648–1656 (2006).
64. J. R. van Beijnum et al., "Tumor angiogenesis is enforced by autocrine regulation of high-mobility group box 1," *Oncogene* **32**(3), 363–374 (2013).
65. G. Helmlinger et al., "Interstitial pH and pO2 gradients in solid tumors in vivo: high-resolution measurements reveal a lack of correlation," *Nat. Med.* **3**(2), 177–182 (1997).
66. S. Anand et al., "Biomodulatory approaches to photodynamic therapy for solid tumors," *Cancer Lett.* **326**(1), 8–16 (2012).

Biographies of the authors are not available.